Evaluation of capacitive micromachined ultrasonic transducers for passive monitoring of microbubble-assisted ultrasound therapies

Ambre Dauba, Jordane Goulas, Laurent Colin, Laurène Jourdain, Benoit Larrat, Jean-Luc Gennisson, Dominique Certon, Anthony Novell

Evaluation of capacitive micromachined ultrasonic transducers for passive monitoring of microbubble-assisted ultrasound therapies

Ambre Dauba, Jordane Goulas, Laurent Colin, Laurène Jourdain, Benoit Larrat, Jean-Luc Gennisson, Dominique Certon, and Anthony Novell

Citation: The Journal of the Acoustical Society of America **148**, 2248 (2020); doi: 10.1121/10.0002096
View online: https://doi.org/10.1121/10.0002096
View Table of Contents: https://asa.scitation.org/toc/jas/148/4
Published by the Acoustical Society of America

JASA ARTICLE

Evaluation of capacitive micromachined ultrasonic transducers for passive monitoring of microbubble-assisted ultrasound therapies

Ambre Dauba,[1] Jordane Goulas,[1] Laurent Colin,[2] Laurène Jourdain,[1] Benoit Larrat,[3] Jean-Luc Gennisson,[1] Dominique Certon,[2] and Anthony Novell[1,a)]

[1]*Université Paris-Saclay, CEA, CNRS, Inserm, BioMaps, Service Hospitalier Frédéric Joliot, Orsay, 91401, France*

[2]*GREMAN CNRS UMR 7347, Université François Rabelais, INSA Centre Val de Loire, Tours, France*

[3]*Université Paris-Saclay, CEA, CNRS, Baobab, NeuroSpin, Gif-sur-Yvette, 91191, France*

ABSTRACT:

Passive cavitation detection can be performed to monitor microbubble activity during brain therapy. Microbubbles under ultrasound exposure generate a response characterized by multiple nonlinear emissions. Here, the wide bandwidth of capacitive micromachined ultrasonic transducers (CMUTs) was exploited to monitor the microbubble signature through a rat skull and a macaque skull. The intrinsic nonlinearity of the CMUTs was characterized in receive mode. Indeed, undesirable nonlinear components generated by the CMUTs must be minimized as they can mask the microbubble harmonic response. The microbubble signature at harmonic and ultra-harmonic components (0.5–6 MHz) was successfully extracted through a rat skull using moderate bias voltage.

 https://doi.org/10.1121/10.0002096

(Received 11 April 2020; revised 3 September 2020; accepted 11 September 2020; published online 21 October 2020)

[Editor: Juan Tu] Pages: 2248–2255

I. INTRODUCTION

To date, the treatment of several diseases is weakened by the presence of vascular endothelial cell barriers.[1,2] Recently, microbubble-assisted focused ultrasound (also called sono-permeabilization) was put forward as a promising therapeutic approach to increase drug delivery in the treatment of brain cancer and other brain disorders.[3,4] Indeed, ultrasound-induced blood-brain barrier (BBB) disruption is a non-invasive and cost-effective method that is currently under clinical investigation.[5,6] Stable cavitation (alternation of expansion and shrinkage) of microbubbles induced by ultrasound near the endothelial barrier directly contributes to tight junction disruption via a push-pull mechanism.[7] While a minimum pressure is required to induce BBB disruption, transmission of an excessive pressure can cause irreversible damage due to violent microbubble activity (inertial cavitation).[8] Transcranial focused ultrasound-induced BBB disruption is particularly challenging due to the high variability in ultrasound transmission through the skull. Therefore, close control of the ultrasound amplitude deposited into the brain is necessary for the clinical use of microbubble-assisted ultrasound therapy. The monitoring of cavitation activity plays this role.

It has been suggested that ultrasonic passive cavitation detection (PCD) is as an efficient method for real-time monitoring of microbubble activity under ultrasound exposure.[9–12] Stable cavitation is characterized by the generation of harmonic components, while inertial cavitation corresponds to broadband emissions.[13] Feedback control algorithms, based on the calculation of inertial and/or stable cavitation doses, have been successfully implemented to adjust the pressure amplitude in real-time and ensure treatment safety.[8,9] Very recently, a new indicator based on the intra-pulse detection of ultra-harmonic events was introduced to discriminate between potentially dangerous and safe ultrasound-induced BBB opening conditions.[14] This intra-pulse monitoring made it possible to observe microbubble destabilization related to the occurrence of unwanted side effects. However, for application in the human brain, PCD transducers are hindered by a lack of sensitivity due to (i) the restricted bandwidth of standard piezoelectric transducers, making it difficult to recover a wide frequency content; and (ii) the attenuation induced by the skull that reduces the signal amplitude (low-pass filter).

In this context, the use of a capacitive micromachined ultrasonic transducer (CMUT) is an interesting option that could solve this issue.[15] A CMUT element is composed of multiple cells, acting as interconnected plate capacitors in which a thin movable plate is placed between the top and bottom electrodes. When an excitation voltage is superimposed on the bias voltage (V_{dc}), the modulation of the electrostatic force between the electrodes induces plate vibrations that result in the generation of an acoustic wave. Conversely, when the biased plate is subjected to an incident

a)Author to whom correspondence should be addressed: anthony.novell@universite-paris-saclay.fr; ORCID: 0000-0003-3649-0956.

https://doi.org/10.1121/10.0002096

ultrasonic wave, a change of capacitance due to plate vibration can be detected to observe the echo. Currently, CMUTs are developed and validated for a large range of biomedical uses, including photoacoustic imaging,[16,17] contrast agent imaging,[18] or as hydrophones.[19] Besides having a low manufacturing cost for mass production, this alternative technology also offers attractive acoustic properties, such as extremely wide frequency bandwidth.[20] We could therefore expect CMUT technology to allow the recovery of nonlinear components (especially far away from the center frequency of the PCD transducer) that are not generally detectable. The contribution of these components would increase the signal amplitude and the robustness of cavitation dose calculations.

Nonetheless, the inherent nonlinear behavior of the CMUT requires consideration for microbubble detection. Indeed, according to the transmit frequency, the bias voltage, and the applied pressure, the signal received by the CMUT can be distorted by undesirable harmonic components induced by the intrinsic nonlinear behavior of the CMUT.[21–23] The CMUT could generate undesirable nonlinear components (at $2f_0$, $3f_0$, $4f_0$, etc.) that would be added to the backscattered signal. These unwanted harmonics would mask the microbubble-specific activity signature, leading to a miscalculation of the stable cavitation dose. When used in its conventional regime (i.e., bias voltage 80% of the collapse voltage), the nonlinearity of the CMUT can generate a second harmonic component that can be three times stronger than the microbubble response.[21] In this condition, the modulation of the bias voltage is an interesting option that can be exploited to reduce the nonlinear CMUT behavior.[24] However, reducing the bias voltage would result in the deterioration of the signal-to-noise ratio (SNR). Thus, a compromise between acceptable nonlinearity and CMUT performance must be found.

To our knowledge, this is the first report investigating the value of using CMUT devices for PCD and the possible degradation of cavitation signals due to the nonlinear behavior of CMUTs. Here, we evaluated *ex vivo* several CMUT configurations for PCD through a rat and a macaque skull. Three CMUT configurations with different cell sizes were developed and characterized to determine the best configuration for PCD. Indeed, the size of the cells modified the operating frequencies and the sensitivity of the transducer. We consolidate that CMUT technology would improve the detection of cavitation events and would outperform competitive technologies in safety monitoring.

II. MATERIALS AND METHODS

A. CMUT configurations

Three single-element CMUTs were developed to detect the backscattered signal from microbubbles at a frequency above 2.5 MHz. As ultrasound-induced BBB disruptions in small animals are typically performed at $\sim$ 1 MHz, CMUTs were initially designed to extract the cavitation signature at harmonic frequency. Briefly, CMUTs were fabricated by using the surface micromachining process, the outlines of which are described in Refs. 25 and 26. Processed wafers were diced to cut the chips to $8 \times 8\,\text{mm}^2$. They were then glued on a circular printed circuit board (PCB) that was specifically designed for this study. Cells were designed with a 400 nm gap and a dimension of $37 \times 37\ \mu\text{m}^2$, $32 \times 32\ \mu\text{m}^2$, or $27 \times 27\ \mu\text{m}^2$. The final receiving aperture of the three CMUT-based passive cavitation detectors was similar (a square of $8 \times 8\,\text{mm}^2$). Cell size modifies the center frequency and the bandwidth of the device. It also affects the sensitivity of the transducer given that larger cells fill a larger active surface area. The active surface area was 50%, 40%, and 35% for the configurations $\text{CMUT}_{37 \times 37\ \mu\text{m}^2}$, $\text{CMUT}_{32 \times 32\ \mu\text{m}^2}$, and $\text{CMUT}_{27 \times 27\ \mu\text{m}^2}$, respectively.

B. Experimental apparatus

Acoustic characterization was performed in order to measure CMUT characteristics (operating frequency and collapse voltage) and estimate their nonlinearity when used in receive mode. First, the bandwidth was estimated using a calibrated hydrophone (HGL200, ONDA Corp., Sunnyvale, CA) by emitting a unipolar pulse (10V_{pp}, pulse width = 150 ns, pulse repetition frequency = 100 Hz; Keysight, AG33210A, Santa Rose, CA). The large size of the CMUT devices makes it particularly challenging to measure CMUT bandwidth in receive mode. To avoid incorrect interpretation, the bandwidth was characterized in emission mode. Accordingly, the excitation conditions fixed for the measurement of the emission performances (low excitation voltage) ensured that CMUT operated in a linear regime. Since the CMUTs were operated as linear devices, reciprocity was met so that both transmitter and receiver bandwidths were assumed to be the same. The signal was then observed on a digital oscilloscope (MSO Series 5 Tektronix, Beaverton, OR) and transferred to a personal computer through a USB port for data analysis (Matlab Release 2018b, The MathWorks, Natick, MA). The collapse voltage was determined by varying V_{dc} from 0 to 120 V (BK Precision 9185, Yorba Linda, CA) and by measuring the signal amplitude. To evaluate CMUT behavior in receive mode, the three different CMUT configurations were placed in a water tank in front of a 1-MHz transducer (V303-SU, Olympus, Tokyo, Japan) used in transmit mode. A 1-MHz, 20-cycle sine wave was transmitted at very low pressure (from 220 to 1100 Pa) to simulate the backscattered signal from the microbubbles.

The ability of CMUTs to detect the signal from circulating microbubbles through a rat skull and a macaque skull was then evaluated. A 100μL bolus of SonoVue microbubbles (Bracco, Milan, Italy) was injected through a water-filled tube ($\phi = 1.5$ mm, flow rate = 6 mL.min^{-1}, dilution in deionized water = 1:1000). Microbubbles were excited at $f_0 = 1$ MHz (peak negative pressure = 270 kPa, pulse duration = 80 cycles, pulse repetition frequency = 10 Hz) using an unfocused disk transducer positioned at 5 cm from the tube (diameter = 16 mm, Imasonic, Voray-sur-l'Ognon, France). A 270 kPa peak negative pressure was chosen to

correspond to a typical acoustic pressure used for safe BBB opening *in vivo*.[8] The number of cycles (i.e., 80) was chosen to: (i) avoid multiple reflections between the PCD transducer and the tube, and (ii) simulate intra-pulse monitoring where timeframes of only a few dozen μs were considered. The pulse repetition frequency (10 Hz) was relatively low to refresh the population of microbubbles circulating in the tube. PCD transducers were placed in a tank filled with degassed water at 6 cm in front of the tube containing flowing microbubbles, and perpendicularly to the transducer transmitting ultrasound at 1 MHz, as shown in Fig. 1. Rat and macaque skulls (parietal bones) were inserted between the tube and the receiving transducer. The skull samples were preserved in degassed water for 48 h prior to experiments. The mean thicknesses of the rat and macaque skulls were 0.4 mm and 3.6 mm, respectively. According to the literature, the amplitude transmission factor at 1 MHz was estimated to be 70% and 25% for the rat[27] and the macaque,[8,28] respectively. Skulls were positioned so that the backscattered signal from the tube crossed the parietal bone with a normal incidence. The PCD transducers were aligned after skull insertion. Briefly, PCD transducers were mounted on a three-axis motorized stage controlled by a software (10 μm accuracy, Image Guided Therapy). To facilitate alignment, the tube was filled with air and the PCD transducers were placed in order to maximize the amplitude of the backscattered signal from the tube. The positioning was checked by two different operators (A.D. and A.N.). Fifty acquisitions were amplified (20 dB, DPR300, JSR Ultrasonics, Pittsford, NY) and acquired on the digital oscilloscope. Each experiment was independently repeated three times. For each acquisition, only PCD transducers were repositioned (i.e., the transmit transducer), but the tube and the skull were not removed to reduce potential sources of variability and allow comparison between receiving transducers.

C. Evaluation method

For each transducer, the limiting frequency at –20 dB (LF-20) was determined on bandwidth measurement to estimate the operating frequency range. The SNR and the fundamental-to-harmonic ratio (FHR) were estimated in receive mode as a function of the V_{dc} and the acoustic pressure. The aim was to find the best compromise between high SNR and a quasi-linear signal (high FHR). The signal detected by the CMUT was converted to the frequency domain (Fast Fourier Transform) to estimate the SNR and the FHR. The SNR corresponded to the ratio of the area under the curve (AUC) at fundamental frequency ($f_0 = 1$ MHz $\pm$ 50 kHz) over the AUC of the baseline noise level obtained at high frequency (>5 MHz). The FHR was obtained from the ratio of AUC at fundamental frequency (1 MHz $\pm$ 50 kHz) over the AUC at second harmonic frequency (2 MHz $\pm$ 50 kHz).

The signal from circulating microbubbles detected by the PCD was averaged by Magnitude Spectrum using a Matlab code. The AUCs of subharmonic, harmonic, and ultra-harmonic contents were calculated as frequencies as specified in Tables I and II. For broadband emissions, the AUCs were calculated by considering six frequency bands of $\pm$ 100 kHz centered at [3.25 + (n – 1) 0.5] MHz (n = 1 to 6). AUC ratios (AUCR) were calculated by comparing the signal from microbubbles to the signal backscattered by the water-filled tube. AUCR are presented as mean $\pm$ standard deviation.

III. RESULTS

A. Characterization of CMUTs in transmit mode

The bandwidth of the three CMUT configurations was characterized in transmit mode. These measurements allowed us to confirm the center frequency of each configuration and to determine the frequency range in which CMUTs were efficient. As shown in Fig. 2(A), the center frequency was 2.7 MHz, 3.0 MHz, and 3.2 MHz for the 37×37 μm^2, 32×32 μm^2, and 27×27 μm^2 configurations, respectively. Interestingly, the LF-20 was between 0.6 and 6.3 MHz for the three CMUT devices. This suggests that the CMUT would be able to detect a wideband nonlinear response. Although a reciprocity between transmitter and receiver bandwidth is expected, we should mention that transmit mode data is only indicating a maximum possible

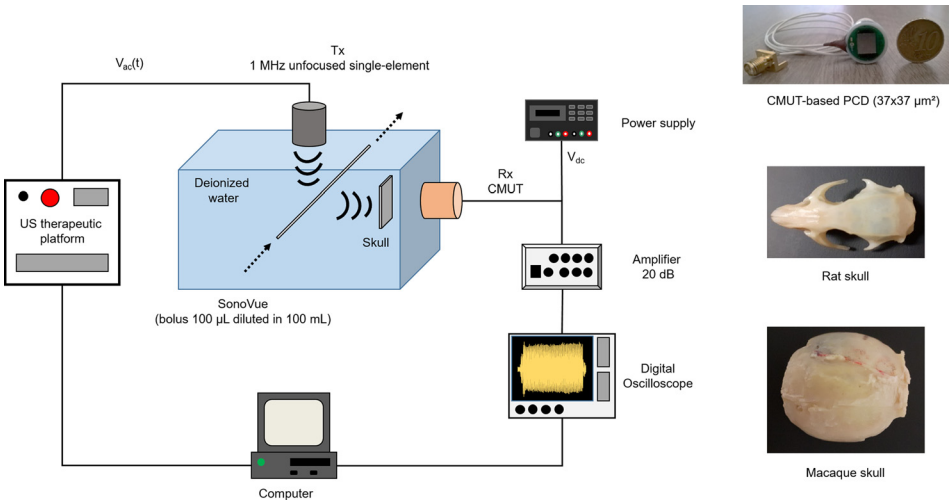

FIG. 1. (Color online) Experimental setup for passive cavitation detection of microbubbles flowing through a skull.

https://doi.org/10.1121/10.0002096

TABLE I. AUC ratio through a rat skull n = 3.

PCD transducer	AUCR subharmonic 0.5 f_0 (dB)	AUCR harmonic (3 f_0 to 6 f_0) (dB)	AUCR ultra-harmonic (2.5 $_0$ to 5.5 f_0) (dB)	AUCR broadband (dB)
CMUT 37 × 37 μm^2	9.7 ± 1.4	24.2 ± 4.5	41.7 ± 5.2	5.2 ± 1.5
CMUT 32 × 32 μm^2	10.3 ± 1.4	18.3 ± 3.3	37.7 ± 3.9	5.1 ± 0.6
CMUT 27 × 27 μm^2	10.3 ± 0.7	23.1 ± 2.0	35.8 ± 0.7	4.4 ± 0.7

bandwidth in receive mode that also takes into account the noise floor.

Figure 2(B) shows the characterization of the collapse voltage V_c for the $CMUT_{37 \times 37\ \mu m^2}$ configuration. V_c (i.e., maximum of the curve) was estimated at $V_{dc} = 35$ V, $V_{dc} = 60$ V, and $V_{dc} = 110$ V for $CMUT_{37 \times 37\ \mu m^2}$, $CMUT_{32 \times 32\ \mu m^2}$, and $CMUT_{27 \times 27\ \mu m^2}$, respectively.

B. Sensitivity and nonlinearity of CMUTs in receive mode

Figure 3(A) shows the SNR of the $CMUT_{37 \times 37\ \mu m^2}$ as a function of V_{dc} and the acoustic pressure (P_{ac}) applied on the transducer. As expected, the SNR increased with P_{ac}, increasing by approximately 6 dB when P_{ac} was doubled. Similarly, the SNR increased up to +18 dB when V_{dc} varied from 0 V to V_c. At the same time, the intrinsic nonlinearity of the CMUT was estimated by calculating the FHR for different V_{dc} and P_{ac}. As shown in Fig. 3(B) for the $CMUT_{37 \times 37\ \mu m^2}$ configuration, a decrease in FHR was observed when V_{dc} and P_{ac} increased, suggesting a stronger nonlinear behavior induced by a partial collapse of the CMUT membrane. This was even when the CMUT was used in receive mode only. Similar trends were observed for $CMUT_{32 \times 32\ \mu m^2}$ and the $CMUT_{27 \times 27\ \mu m^2}$ (data not shown). Figures 3(C) through 3(H) illustrate the compromise between the intrinsic nonlinearity and the sensitivity performance of the CMUT devices. Examples of received pressure signals (middle line) and corresponding frequency spectra (bottom line) are displayed for $V_{dc} = 0.3$ V_c (C, F), $V_{dc} = 0.6$ V_c (D, G), and $V_{dc} = 0.9$ V_c (E, H) at a pressure of 1.1 kPa. While a high SNR can be observed at $V_{dc} = 0.9$ V_c, the corresponding spectrum shows the generation of undesirable harmonic components at 2 f_0, 3 f_0, and 4 f_0 that would prevent microbubble detection. Therefore, the intrinsic nonlinearity of the CMUTs must be avoided, given it could mask the microbubble response. Previously in Ref. 21, we demonstrated that an FHR of 30 dB was suitable for extracting the nonlinear response of contrast agents. Consequently, for the remainder of this study, all CMUT configurations were used at $V_{dc} = 0.6$ V_c in order to maximize the sensitivity in receive mode while maintaining a reasonable level of nonlinearity (FHR > 30 dB).

C. Evaluation of CMUTs for PCD

Initially, the ability of the CMUTs to detect the signal from microbubbles was evaluated in skull absence. Frequency spectra are displayed in Fig. 4(A) for the $CMUT_{37 \times 37\ \mu m^2}$-based PCD. We observed that CMUTs allowed signal recovery from microbubbles with a high sensitivity of up to the ninth harmonic (see Tables S1 and S2). Interestingly, ultra-harmonic components were particularly detectable using the $CMUT_{37 \times 37\ \mu m^2}$ configuration. These components tend to be difficult to detect as they are weaker than harmonics. For example, between 3 and 6 MHz, ultra-harmonic peaks were approximately 10 to 15 dB lower than those for harmonics.

Next, the influence of the skull on the nonlinear signal detection was evaluated by inserting the rat and macaque skulls between the tube and the PCD transducer. Examples of frequency spectra are given in Figs. 4(B) and 4(C) for $CMUT_{37 \times 37\ \mu m^2}$. As expected, the presence of the skull considerably attenuated the high frequency components. Using the CMUT, a peak frequency was detectable up to the sixth and the third harmonic through the rat and macaque skulls, respectively. Quantitative results (AUCR) are given in Tables I and II. For the rat skull, the detection of both harmonic (stable cavitation) and ultra-harmonic content was improved using the $CMUT_{37 \times 37\ \mu m^2}$ configuration (up to +5.9 dB compared to the other configurations). Interestingly, the AUCR of detected subharmonic components remained at approximately 10 dB for all transducers. These results confirmed that CMUTs were able to detect a wideband of frequency content (i.e., from 0.5 f_0 to 6 f_0) through the rat skull. The detection of broadband signal, corresponding to inertial cavitation, through the rat skull was approximately the same for all CMUT devices.

It is important to mention that CMUT-based PCD developed in this study was not designed for macaque application. Given the strong attenuation of the skull (>75% amplitude at 1 MHz), the frequency used for BBB opening in non-human primates is generally lower (typically around 0.5 MHz) to allow the transmission of ultrasound energy. Therefore,

TABLE II. AUC ratio through a macaque skull n = 3.

PCD transducer	AUCR subharmonic 0.5 f_0 (dB)	AUCR harmonic (3 f_0) (dB)	AUCR ultra-harmonic (2.5 f_0) (dB)	AUCR broadband (dB)
CMUT 37 × 37 μm^2	14.4 ± 1.8	−1.8 ± 0.7	7.9 ± 1.2	2.2 ± 0.5

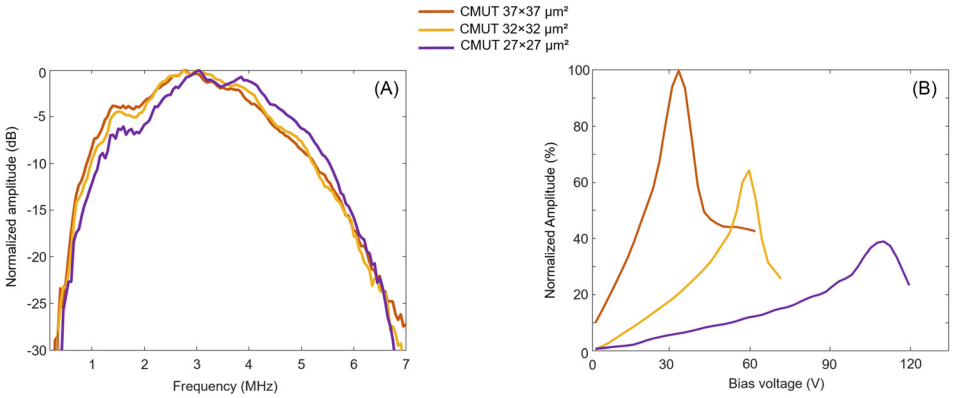

FIG. 2. (Color online) (A) Comparison of bandwidth measurements for the three CMUT configurations designed in this study. (B) Sensitivity in transmit mode as a function of the bias voltage for the three CMUT devices.

CMUT-based PCD centered around 1.25–1.5 MHz would be more suitable for this use. Although our configurations were not optimal, we decided to evaluate the CMUT with the lowest center frequency (i.e., $CMUT_{37\times37\,\mu m^2}$) through the macaque skull. Results showed that only the subharmonic, the harmonic at $3f_0$, and the ultra-harmonic at 2.5 f_0 components were detectable.

IV. DISCUSSION AND CONCLUSION

We validate here a new application for CMUT technology in the monitoring of cavitation-based ultrasound therapies that may include HIFU, sono-permeabilization, or BBB opening. We have demonstrated that CMUTs are able to detect broadband cavitation signal through rat and macaque skulls. Used in receive mode only, immersed CMUTs provide an inherent broadband response.[29] Here in our study, this resulted in a stronger sensitivity in the high frequency content (i.e., frequency $>$ 3.5 MHz for the rat skull) for the CMUT devices evaluated. Although very similar acoustic performances were found for the three configurations, the $CMUT_{37\times37\ \mu m^2}$ configuration was the most promising for small animal application (+5.9 dB in harmonic and +5.9 dB in ultra-harmonic contents compared to the other configurations). This better performance could be explained by the larger active surface area (i.e., 50%) and by the center frequency of this configuration (2.7 MHz), allowing an excellent detection of the ultra-harmonic component at 2.5 f_0. The development of efficient PCD for use in rodents is essential for the improvement of ultrasound therapy protocols used in various pathological models (e.g., glioblastoma, Alzheimer's, Parkinson's). It is additionally required for the development of robust feedback control loops based on the enhanced detection of microbubble acoustic signatures.

Unfortunately, a direct comparison of CMUT technology with another existing technology (piezoelectric, piezocomposite, or polyvinylidene fluoride) was not possible; another PCD transducer with an equivalent aperture ($8\times8\,mm^2$) was not available in the lab. Furthermore, only one skull from each species was evaluated in this pilot study. The high inter-individual variability of skull attenuation (especially for the macaque) could affect the findings of this study. For example, a thicker skull bone would render the detection of the high frequency content more difficult.

Our CMUT devices allowed the detection of cavitation signal through the rat skull from 0.5 f_0 to 6 f_0 [Fig. 4(B)]. This result is particularly encouraging regarding the literature. For example, Sun *et al.* reported an acoustic emission recording from f_0 to $4f_0$ through the rat skull using an elliptical air-backed PCD.[11] In another study, Chu *et al.* calculated the cavitation dose in rat brain from $0.5f_0$ to $2.5f_0$ using a

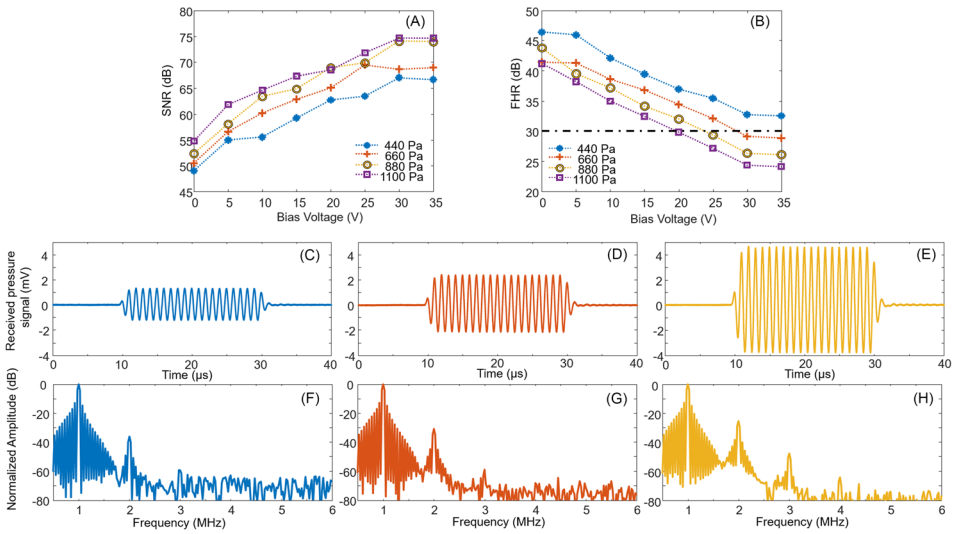

FIG. 3. (Color online) Sensitivity and nonlinearity of the $CMUT_{37\times37\,\mu m^2}$ device used in receive mode. Variation of the signal-to-noise ratio (SNR) (A) and the fundamental-to-harmonic ratio (FHR) (B) as a function of the bias voltage and the acoustic pressure applied at 1 MHz. Examples of receive pressure signals (middle line) and corresponding frequency spectra (bottom line) are displayed for $V_{dc} = 0.3\ V_c$ (C, F), $V_{dc} = 0.6\ V_c$ (D, G), and $V_{dc} = 0.9\ V_c$ (E, H) at a pressure of 1.1 kPa.

https://doi.org/10.1121/10.0002096

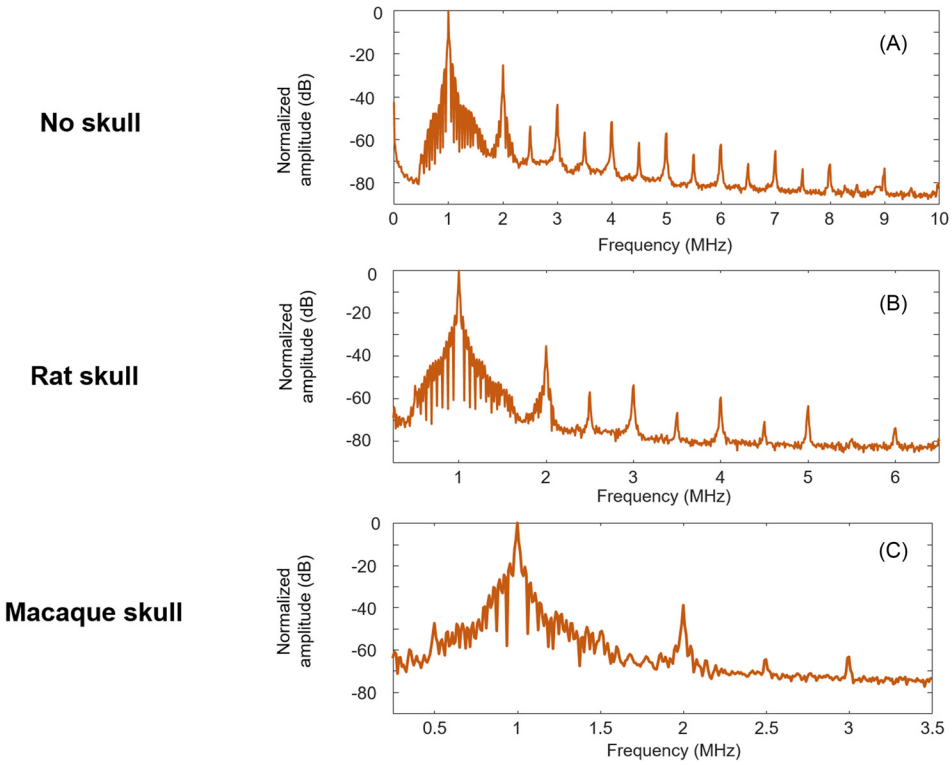

FIG. 4. (Color online) Examples of the frequency responses from flowing microbubbles (Tx: 1 MHz, 270 kPa, and 80 cycles) detected by the $CMUT_{37\times37\mu m2}$ device without a skull (A), through a rat skull (B), and through a macaque skull (C).

needle hydrophone.[30] As previously discussed, the CMUT-based PCDs developed here were not optimized for the macaque application. Despite this, harmonics up to $3f_0$ (3.0 MHz) were detectable through the skull. In comparison, Kamimura *et al.* were able to detect cavitation signal from $0.5f_0$ (0.25 MHz) to $4.5f_0$ (2.25 MHz) using a piezocomposite PCD[8] and an emission at lower frequency (0.5 MHz). Under the same conditions, a superiority of CMUT technology would be expected.

We deliberately chose to apply a bias voltage of 60% V_c. This was in order to maintain the intrinsic nonlinearity of the CMUT as low as acceptable at the expense of decreased sensitivity. This choice was reasoned by the need to maintain a low level of undesirable harmonic components—at $2f_0$, $3f_0$, $4f_0$, $5f_0$, etc.—to allow the detection of the microbubble harmonic response. The determination of stable cavitation dose is based on the level of harmonics generated during ultrasound exposure. Therefore, V_{dc} must be carefully selected, as the intrinsic nonlinearity of the CMUT can skew the calculation of this indicator typically used to guarantee an efficient BBB opening. Nevertheless, we recently demonstrated that the intra-pulse monitoring of ultra-harmonic content is another relevant approach for ensuring efficient and safe BBB opening.[14] Ultra-harmonics correspond to nonlinear oscillations of microbubbles and are not generated by the CMUT. Therefore, it would be advantageous to use CMUTs for measuring these critical spectral components. If the monitoring of stable cavitation dose is not required, we encourage the application of a maximum V_{dc} (i.e., $V_{dc} = V_c$) to further increase CMUT sensitivity in receive mode. This would not affect the estimation of inertial cavitation dose that is based on the detection of broadband content in microbubble responses.

Undesirable harmonics are also generated by the nonlinear propagation of ultrasound waves through various media. In our experiments, the reflection from the tube wall masked the microbubbles response at $2f_0$. This recapitulates *in vivo* conditions, where the echo from the skull is often masking the backscattered signal from microbubbles at $2f_0$. For this reason, PCD transducers are generally designed to recover frequencies above $2f_0$. Therefore, the signal at $2f_0$ was not taken into account in our AUCR calculations. An additional peak at $1.5f_0$ was also not considered in our results. Although the Fast Fourier Transform was calculated on the full backscattered signal of 80 μs, it was not possible to extract this peak in our frequency spectra as shown in Fig. 4. Increasing the number of cycles would have induced multiple reflections within the skull that would have impaired the spectral analysis.

Attenuation could have limited exploitation of the signal received in high frequency range (as shown in macaque skull data), meaning that the gain from the CMUT may not actually have been so profound. However, the real limitation was the noise floor of the system; a standard electronic receiving circuit was used. Future work will be focused on the development of dedicated amplifiers that can be directly integrated in CMUT PCBs. CMUTs are intrinsically noiseless technologies since receivers are "pure" capacitors with very low levels of thermal-mechanical noise.[31] The use of dedicated amplifiers would provide a substantial improvement in SNR.

The results obtained in this study encourage us in the perusal of our *in vivo* investigation and in developing

CMUT-based PCD for validation in large animals. Recent advances in the CMUT fabrication process allow the consideration of new transducer design, including flexible devices and multi-frequency transducers that could benefit real-time monitoring.[32] The demonstration of single-element CMUT-based PCD is a first step in cavitation monitoring. Besides, recent passive acoustic mapping (PAM) techniques have been developed to provide spatial distribution information on microbubble activity.[33,34] Spatially resolved monitoring of cavitation emissions can be obtained using commercial imaging probes[35] or customized arrays.[36,37] A CMUT probe composed of multiple arrays (such as the one developed by Ref. 38) could be an interesting option for simultaneous therapy and cavitation monitoring.

ACKNOWLEDGMENTS

This work was partly funded by ANR DROPMUT (Grant No. ANR-19-CE19-0011) and France Life Imaging (Grant No. ANR-11-INBS-0006). The authors would like to acknowledge Georges Willoquet, Flavien Barcella, and Nicolas Sénégond for their technical assistance. We thank Jackie Butterworth for manuscript proofreading.

[1]W. M. Pardridge, "CSF, blood-brain barrier, and brain drug delivery," Expert Opin. Drug Deliv. **13**, 963–975 (2016).
[2]A. Bhowmik, R. Khan, and M. K. Ghosh, "Blood brain barrier: A challenge for effectual therapy of brain tumors," Biomed. Res. Int. **2015**, 320941 (2015).
[3]K. H. Song, B. K. Harvey, and M. A. Borden, "State-of-the-art of microbubble-assisted blood-brain barrier disruption," Theranostics **8**, 4393–4408 (2018).
[4]Z. Deng, Z. Sheng, and F. Yan, "Ultrasound-induced blood-brain-barrier opening enhances anticancer efficacy in the treatment of glioblastoma: Current status and future prospects," J. Oncol. **2019**, 2345203 (2019).
[5]T. Mainprize, N. Lipsman, Y. Huang, Y. Meng, A. Bethune, S. Ironside, C. Heyn, R. Alkins, M. Trudeau, A. Sahgal, J. Perry, and K. Hynynen, "Blood-brain barrier opening in primary brain tumors with non-invasive MR-guided focused ultrasound: A clinical safety and feasibility study," Sci. Rep. **9**, 321 (2019).
[6]A. Idbaih, M. Canney, L. Belin, C. Desseaux, A. Vignot, G. Bouchoux, N. Asquier, B. Law-Ye, D. Leclercq, A. Bissery, Y. De Rycke, C. Trosch, L. Capelle, M. Sanson, K. Hoang-Xuan, C. Dehais, C. Houillier, F. Laigle-Donadey, B. Mathon, A. Andre, C. Lafon, J. Y. Chapelon, J. Y. Delattre, and A. Carpentier, "Safety and feasibility of repeated and transient blood-brain barrier disruption by pulsed ultrasound in patients with recurrent glioblastoma," Clin. Cancer Res. **25**, 3793–3801 (2019).
[7]N. McDannold, N. Vykhodtseva, and K. Hynynen, "Targeted disruption of the blood-brain barrier with focused ultrasound: Association with cavitation activity," Phys. Med. Biol. **51**, 793–807 (2006).
[8]H. A. Kamimura, J. Flament, J. Valette, A. Cafarelli, R. Aron Badin, P. Hantraye, and B. Larrat, "Feedback control of microbubble cavitation for ultrasound-mediated blood-brain barrier disruption in non-human primates under magnetic resonance guidance," J. Cereb. Blood Flow Metab. **39**, 1191–1203 (2019).
[9]M. A. O'Reilly and K. Hynynen, "Blood-brain barrier: Real-time feedback-controlled focused ultrasound disruption by using an acoustic emissions-based controller," Radiology **263**, 96–106 (2012).
[10]S. Y. Wu, C. Aurup, C. S. Sanchez, J. Grondin, W. Zheng, H. Kamimura, V. P. Ferrera, and E. E. Konofagou, "Efficient blood-brain barrier opening in primates with neuronavigation-guided ultrasound and real-time acoustic mapping," Sci. Rep. **8**, 7978 (2018).
[11]T. Sun, Y. Zhang, C. Power, P. M. Alexander, J. T. Sutton, M. Aryal, N. Vykhodtseva, E. L. Miller, and N. J. McDannold, "Closed-loop control of targeted ultrasound drug delivery across the blood-brain/tumor barriers in a rat glioma model," Proc. Natl. Acad. Sci. U.S.A. **114**, E10281–E10290 (2017).
[12]M. A. O'Reilly and K. Hynynen, "A PVDF receiver for ultrasound monitoring of transcranial focused ultrasound therapy," IEEE Trans. Biomed. Eng. **57**, 2286–2294 (2010).
[13]Y. S. Tung, J. J. Choi, B. Baseri, and E. E. Konofagou, "Identifying the inertial cavitation threshold and skull effects in a vessel phantom using focused ultrasound and microbubbles," Ultrasound Med. Biol. **36**, 840–852 (2010).
[14]A. Novell, H. Kamimura, A. Cafarelli, M. Gerstenmayer, J. Flament, J. Valette, P. Agou, A. Conti, E. Selingue, R. Aron Badin, P. Hantraye, and B. Larrat, "A new safety index based on intrapulse monitoring of ultraharmonic cavitation during ultrasound-induced blood-brain barrier opening procedures," Sci. Rep. **10**, 10088 (2020).
[15]B. T. Khuri-Yakub and O. Oralkan, "Capacitive micromachined ultrasonic transducers for medical imaging and therapy," J. Micromech. Microeng. **21**, 54004–54014 (2011).
[16]S. Vaithilingam, T. J. Ma, Y. Furukawa, I. O. Wygant, X. Zhuang, A. De La Zerda, O. Oralkan, A. Kamaya, S. S. Gambhir, R. B. Jeffrey, Jr., and B. T. Khuri-Yakub, "Three-dimensional photoacoustic imaging using a two-dimensional CMUT array," IEEE Trans. Ultrason. Ferroelectr. Freq. Control **56**, 2411–2419 (2009).
[17]M. Vallet, F. Varray, J. Boutet, J. M. Dinten, G. Caliano, A. S. Savoia, and D. Vray, "Quantitative comparison of PZT and CMUT probes for photoacoustic imaging: Experimental validation," Photoacoustics **8**, 48–58 (2017).
[18]A. Novell, J. M. Escoffre, and A. Bouakaz, "Second harmonic and subharmonic for non-linear wideband contrast imaging using a capacitive micromachined ultrasonic transducer array," Ultrasound Med. Biol. **39**, 1500–1512 (2013).
[19]P. Cristman, O. Oralkan, X. Zhuang, T. J. Ma, S. Vaithilingam, T. Carver, I. O. Wygant, and B. T. Khuri-Yakub, editors. "A 2D CMUT hydrophone array: Characterization results," in *Proceedings of IEEE Ultrasonics Symposium*, Rome (2009).
[20]A. Boulmé, S. Ngo, J. Minonzio, M. Legros, M. Talmant, P. Laugier, and D. Certon, "A capacitive micromachined ultrasonic transducer probe for assessment of cortical bone," IEEE Trans. Ultrason. Ferroelectr. Freq. Control **61**, 710–723 (2014).
[21]A. Novell, M. Legros, N. Felix, and A. Bouakaz, "Exploitation of capacitive micromachined transducers for nonlinear ultrasound imaging," IEEE Trans. Ultrason. Ferroelectr. Freq. Control **56**, 2733–2743 (2009).
[22]A. Lohfink and P. C. Eccardt, "Investigation of nonlinear CMUT behavior," in *Proceedings of IEEE Ultrasonics Symposium* (2005), pp. 585–588.
[23]A. Novell, M. Legros, J. M. Gregoire, P. A. Dayton, and A. Bouakaz, "Evaluation of bias voltage modulation sequence for nonlinear contrast agent imaging using a capacitive micromachined ultrasonic transducer array," Phys. Med. Biol. **59**, 4879–4896 (2014).
[24]A. Novell, C. B. Arena, S. Kasoji, and P. A. Dayton, "Optimization of multi-pulse sequences for nonlinear contrast agent imaging using a CMUT array," Phys. Medic. Biol. **60**, 3111–3127 (2015).
[25]C. Meynier, F. Teston, and D. Certon, "A multiscale model for array of capacitive micromachined ultrasonic transducers," J. Acoust. Soc. Am. **128**, 2549–2561 (2010).
[26]J. Heller, A. Boulme, D. Alquier, S. Ngo, and D. Certon, "Performance evaluation of CMUT-based ultrasonic transformers for galvanic isolation," IEEE Trans. Ultrason. Ferroelectr. Freq. Control **65**, 617–629 (2018).
[27]M. Gerstenmayer, B. Fellah, R. Magnin, E. Selingue, and B. Larrat, "Acoustic transmission factor through the rat skull as a function of body mass, frequency and position," Ultrasound Med. Biol. **44**, 2336–2344 (2018).
[28]S. Y. Wu, Y. S. Tung, F. Marquet, M. Downs, C. Sanchez, C. Chen, V. Ferrera, and E. Konofagou, "Transcranial cavitation detection in primates during blood-brain barrier opening: A performance assessment study," IEEE Trans. Ultrason. Ferroelectr. Freq. Control **61**, 966–978 (2014).
[29]A. Novell, C. B. Arena, O. Oralkan, and P. A. Dayton, "Wideband acoustic activation and detection of droplet vaporization events using a capacitive micromachined ultrasonic transducer," J. Acoust. Soc. Am. **139**, 3193–3198 (2016).
[30]P. C. Chu, W. Y. Chai, C. H. Tsai, S. T. Kang, C. K. Yeh, and H. L. Liu, "Focused ultrasound-induced blood-brain barrier opening: Association

https://doi.org/10.1121/10.0002096

with mechanical index and cavitation index analyzed by dynamic contrast-enhanced magnetic-resonance imaging," Sci. Rep. **6**, 33264 (2016).
[31]G. Gurun, M. Hochman, P. Hasler, and F. L. Degertekin, "Thermal-mechanical-noise-based CMUT characterization and sensing," IEEE Trans. Ultrason. Ferroelectr. Freq. Control **59**, 1267–1275 (2012).
[32]K. Brenner, A. S. Ergun, K. Firouzi, M. F. Rasmussen, Q. Stedman, and B. P. Khuri-Yakub, "Advances in capacitive micromachined ultrasonic transducers," Micromachines (Basel) **10**(2), 152 (2019).
[33]K. J. Haworth, V. A. Salgaonkar, N. M. Corregan, C. K. Holland, and T. D. Mast, "Using passive cavitation images to classify high-intensity focused ultrasound lesions," Ultrasound Med. Biol. **41**, 2420–2434 (2015).
[34]C. Coviello, R. Kozick, J. Choi, M. Gyongy, C. Jensen, P. P. Smith, and C. C. Coussios, "Passive acoustic mapping utilizing optimal beamforming in ultrasound therapy monitoring," J. Acoust. Soc. Am. **137**, 2573–2585 (2015).
[35]Y. Yang, X. Zhang, D. Ye, R. Laforest, J. Williamson, Y. Liu, and H. Chen, "Cavitation dose painting for focused ultrasound-induced blood-brain barrier disruption," Sci. Rep. **9**, 2840 (2019).
[36]R. M. Jones, M. A. O'Reilly, and K. Hynynen, "Experimental demonstration of passive acoustic imaging in the human skull cavity using ct-based aberration corrections," Med. Phys. **42**, 4385–4400 (2015).
[37]C. Crake, S. T. Brinker, C. M. Coviello, M. S. Livingstone, and N. J. McDannold, "A dual-mode hemispherical sparse array for 3D passive acoustic mapping and skull localization within a clinical MRI guided focused ultrasound device," Phys. Med. Biol. **63**, 065008 (2018).
[38]D. Gross, C. Coutier, M. Legros, A. Bouakaz, and D. Certon, "A CMUT probe for ultrasound-guided focused ultrasound targeted therapy," IEEE Trans. Ultrason. Ferroelectr. Freq. Control **62**, 1145–1160 (2015).